Quantum Simulation of the Schrodinger Equation

Ayush Singhal
National Institute of Science Education and Research
Bhubaneswar, Odisha 751005, India
4th year, Integrated M.Sc. Physics
Roll No.: 2011042
(Dated: May 9, 2024)

This report presents the quantum simulation of the Schrödinger equation for diverse one-dimensional potentials using Qiskit, a platform for quantum computing. By leveraging the unique capabilities of quantum computing, specifically utilizing six qubits, simulations were conducted for a range of potentials, including the free particle, infinite square well, simple harmonic oscillator (SHO), quantum tunnelling, and two-particle system. The Schrödinger equation, a fundamental equation in quantum mechanics, describes the behavior of quantum systems. By applying quantum algorithms, the simulations provided insights into the behaviour and properties of these potentials in the quantum realm.

I. INTRODUCTION

Quantum mechanics, with its probabilistic nature and peculiar phenomena, has long fascinated physicists and researchers alike. At the heart of this revolutionary theory lies the Schrödinger equation, a cornerstone of quantum mechanics that governs the behavior of quantum systems. The solutions to this equation provide profound insights into the properties and dynamics of particles at the quantum level.

In recent years, the advent of quantum computing has opened up new avenues for exploring and understanding quantum phenomena. Quantum simulators, in particular, offer a promising approach to studying complex quantum systems that are challenging to analyze using classical computational methods. These simulators harness the principles of quantum mechanics to model the behavior of quantum systems, providing a platform for investigating a wide range of physical phenomena.

In this report, we delve into the quantum simulation of the Schrödinger equation for various one-dimensional potentials. By employing Qiskit, a leading quantum computing framework, we aim to explore the behavior of quantum systems under different potential landscapes. Specifically, we focus on potentials such as the free particle, the infinite square well, the simple harmonic oscillator (SHO), quantum tunneling phenomena, and step potentials.

The choice of these potentials is motivated by their significance in quantum mechanics and their relevance to real-world physical systems. Through quantum simulation, we seek to unravel the intricate dynamics and properties of these potentials in the quantum domain. Leveraging six qubits, we conduct simulations that offer insights into phenomena such as confinement, tunneling, and energy quantization, shedding light on the quantum behavior of particles under diverse conditions.

By simulating these potentials on a quantum computing platform, we aim to demonstrate the potential of quantum computing as a powerful tool for investigating quantum systems. The results of our simulations not only contribute to our understanding of fundamental quantum phenomena but also pave the way for the development of future quantum technologies and applications.

In the subsequent sections of this report, we will detail the methodology employed for quantum simulation, present our findings for each potential, and discuss the implications of our results. Through this exploration, we hope to highlight the promise and potential of quantum simulation in advancing our understanding of the quantum world.

II. HOW QUANTUM COMPUTING WORKS

Quantum computing harnesses the principles of quantum mechanics to perform computational tasks in fundamentally new ways, offering the potential for significant advancements in fields ranging from cryptography to drug discovery. At its core, quantum computing relies on the quantum bits, or qubits, as the fundamental units of information processing. Unlike classical bits, which can only exist in a state of 0 or 1, qubits can exist in a superposition of both states simultaneously, exponentially increasing the computational power of a quantum computer.

A. Qubits

Quantum bits, or qubits, are the fundamental units of information in a quantum computer. A qubit is analogous to a quantum state of a half-spin particle and can be described by the superposition:

$$|\psi\rangle = \alpha|0\rangle + \beta|1\rangle$$

where α and β are complex coefficients. The probabilities of the qubit's state being measured as $|0\rangle$ or $|1\rangle$ are given by $|\alpha|^2$ and $|\beta|^2$ respectively, and they satisfy the normalization condition:

$$|\alpha|^2 + |\beta|^2 = 1.$$

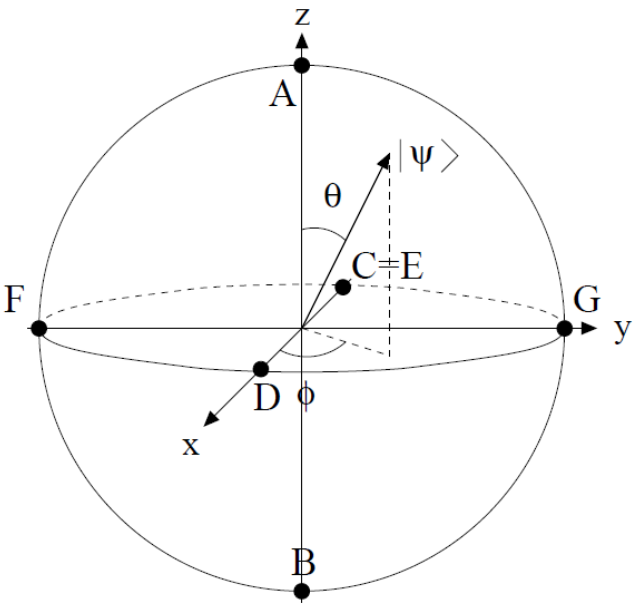

FIG. 1: Visualization of a qubit on the Bloch Sphere.

This is effectively visualized using the Bloch Sphere (fig 1), where the state $|\psi\rangle$ is represented as:

$$|\psi\rangle = \cos\left(\frac{\theta}{2}\right)|0\rangle + e^{i\phi}\sin\left(\frac{\theta}{2}\right)|1\rangle,$$

with θ being the polar angle affecting the measurement probabilities and ϕ the azimuthal phase angle.

B. Superposition

In quantum mechanics, superposition allows particles to exist in multiple states simultaneously until they are observed. This principle is central to quantum computing, where qubits can be in a state of $|0\rangle$, $|1\rangle$, or any combination of both states, represented by a complex vector in a two-dimensional Hilbert space. This ability to simultaneously represent multiple possibilities enables quantum computers to perform parallel computations on a massive scale.

C. Entanglement

Entanglement is another quintessential feature of quantum mechanics that distinguishes quantum computing from classical computing. When qubits become entangled, the state of one qubit becomes correlated with the state of another, regardless of the distance between them. This phenomenon enables quantum computers to perform operations on multiple qubits simultaneously, leading to a higher degree of computational efficiency and complexity.

D. Quantum Gates and Quantum Circuits

Analogous to classical logic gates, quantum gates are fundamental building blocks for quantum circuits, which manipulate qubits to perform computational tasks. These gates operate on qubits, transforming their states based on the principles of quantum mechanics. Common quantum gates include the Hadamard gate, which creates superposition, the Pauli-X gate (also known as the quantum NOT gate), and the CNOT (Controlled-NOT) gate, which introduces entanglement between qubits.

E. Quantum Algorithms

Quantum algorithms are algorithms designed to exploit the unique properties of quantum mechanics to solve specific computational problems more efficiently than their classical counterparts. Prominent examples include Shor's algorithm for integer factorization and Grover's algorithm for unstructured search problems. These algorithms leverage quantum parallelism and interference to achieve exponential speedup over classical algorithms for certain tasks.

F. Decoherence and Error Correction

Despite the potential advantages of quantum computing, qubits are inherently fragile and susceptible to environmental noise, leading to decoherence—the loss of quantum coherence over time. Decoherence poses a significant challenge to quantum computation, as it can introduce errors and limit the reliability of quantum calculations. To address this issue, researchers are developing quantum error correction techniques that involve encoding quantum information redundantly to protect against errors caused by decoherence and other noise sources.

III. SIMULATION OF THE 1D SHRODINGER EQUATION USING QISKIT

We are simulating the time evolution for one-dimensional single-particle quantum systems on quantum computers. We will be using the python library for Quantum Information Science (QISKit). Recalling the time-dependent schrodinger equation

$$H|\psi(t)\rangle = \imath\hbar\frac{\partial}{\partial t}|\psi(t)\rangle \tag{1}$$

For time-independent Hamiltonian H,

$$H = K + V = \frac{p^2}{2m} + V \tag{2}$$

we have

$$|\psi(t)\rangle = \mathbf{e}^{-\imath Ht}|\psi(0)\rangle \tag{3}$$

By Trotter Formula, we have

$$|\psi(t)\rangle = \mathbf{e}^{-\imath(K+V)t}|\psi(0)\rangle = \left(\mathbf{e}^{-\imath K\Delta t}\mathbf{e}^{-\imath V\Delta t}\mathbf{e}^{O\left(\Delta t^2\right)}\right)^{\frac{t}{\Delta t}}|\psi(0)\rangle \tag{4}$$

A. Initialization

We initialize the wavefunction over a series of N qubits. Therefore, we confine the particle to the positions range $-d \leq x \leq d$. We take equal intervals of

$$\Delta = \frac{2d}{2^N} \tag{5}$$

where 2^N is the number of intervals. The wavefunction can then be discretised by:

$$\sum_{k=0}^{2^N-1} c_k(t)|k\rangle = \frac{1}{\mathcal{N}}\sum_{k=0}^{2^N-1}\psi(x_k,t)|k\rangle \tag{6}$$

where, $|k\rangle$ is the computational basis, and

$$x_k \doteq -d + \left(k+\frac{1}{2}\right)\Delta \tag{7}$$

and, the normalization constant $\mathcal{N}$

$$\mathcal{N} \equiv \sqrt{\sum_{k=0}^{2^N-1}|\psi(x_k,t)|^2} \tag{8}$$

B. The Kinetic Operator

The Kinetic part of the hamiltonian

$$K = \frac{p^2}{2m} = -\frac{\hbar^2}{2m}\frac{d^2}{dx^2} \tag{9}$$

where, the momentum operator

$$p = \imath\hbar\frac{d}{dx} \tag{10}$$

The position x and momentum p operators are related by the Quantum Fourier Transform F as

$$p = FxF^\dagger \tag{11}$$

Then, the Kinetic Energy Operator becomes

$$\mathbf{e}^{-\imath K\Delta t/\hbar} = F\mathbf{e}^{-\imath x^2\Delta t/2m\hbar}F^\dagger \tag{12}$$

Any integer k can be written in Boolean form as

$$k = k_{n-1}2^{n-1} + \cdots + k_1 2^1 + k_0 2^0; \quad k_i \in \{0,1\} \tag{13}$$

By Eq(7), we can write the position x as

$$x = -d + \left[\left(\sum_{j=0}^{N-1} k_j 2^j\right) + \frac{1}{2}\right]\Delta = \alpha\sum_{j=0}^{N-1}\left(k_j 2^j + \beta\right) \tag{14}$$

where,

$$\alpha = \Delta \tag{15}$$

and,

$$\beta = \frac{-d+\Delta/2}{\Delta N} = \frac{1-2^N}{2N} \tag{16}$$

Therefore,

$$\mathbf{e}^{-\imath x^2\Delta t/2m\hbar} = \prod_{j,l=0}^{N-1}\mathbf{e}^{-\imath\gamma(k_j 2^j+\beta)(k_l+2^l+\beta)} \tag{17}$$

where,

$$\gamma = \frac{\alpha^2\Delta t}{2m\hbar} \tag{18}$$

To write operator (17) in the Ising format, we make the replacement

$$k_i = \frac{I - Z_i}{2}; \quad Z_i \in \{-1,1\} \tag{19}$$

Then, we have

$$\begin{aligned}&(k_j 2^j+\beta)(k_l 2^l+\beta)\\ &= \frac{1}{\gamma}\left[(\theta_{j,l}+\theta_j+\theta_l+\beta^2)I - (\theta_{j,l}+\theta_j)Z_j - (\theta_{j,l}+\theta_l)Z_l + \theta_{j,l}Z_jZ_l\right]\end{aligned} \tag{2}$$

where, I is the identity operator and Z_i is the Pauli-Z operator at qubit i, and

$$\theta_{j,l} = \theta_{l,j} = \gamma\, 2^{j+l-2} \tag{21}$$

and,

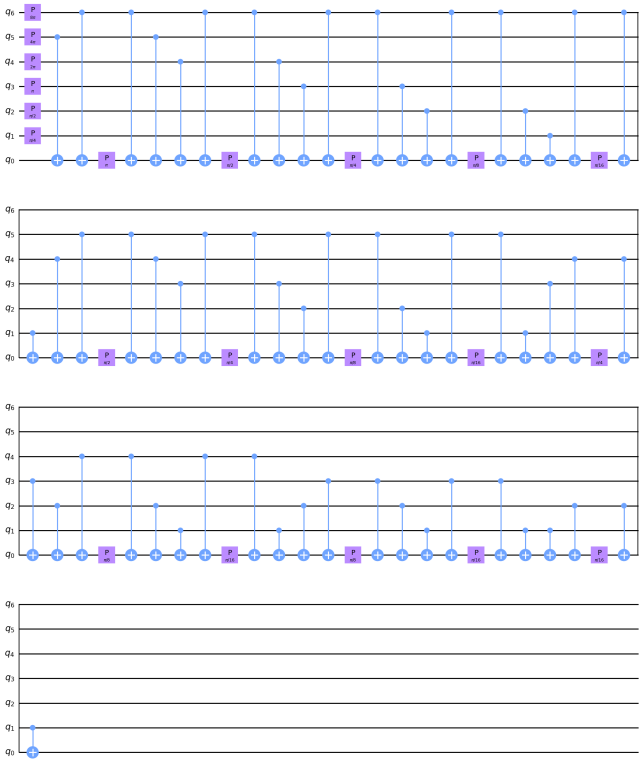

FIG. 2: The Quantum Circuit for kinetic energy operator for 6-qubit system

$$\theta_j = \gamma\,\beta\,2^{j-1} \tag{22}$$

Substituting by Eq(20) into Eq(17) to give

$$\mathbf{e}^{-\imath x^2\Delta t/2m\hbar} = \prod_{j,l=0}^{N-1} \mathbf{e}^{\imath(\theta_{j,l}+\theta_j)Z_j}\ \mathbf{e}^{-\imath\theta_{j,l}Z_jZ_l}\ \mathbf{e}^{\imath(\theta_{j,l}+\theta_l)Z_l} \tag{23}$$

where, we have ignored the global phase factor. By Eq(12), the Kinetic operator becomes

$$\mathbf{e}^{-\imath K\Delta t/\hbar} = \prod_{j,l=0}^{N-1} F\,\mathbf{e}^{\imath(\theta_{j,l}+\theta_j)Z_j}\ \mathbf{e}^{-\imath\theta_{j,l}Z_jZ_l}\ \mathbf{e}^{\imath(\theta_{j,l}+\theta_l)Z_l}\ F^\dagger \tag{24}$$

The Quantum Circuit for kinetic energy operator for 6-qubit system is shown in fig 2

C. The Quantum Fourier Transform

Suppose we have two vectors

$$X = \{x_0, x_1, \cdots, x_k, \cdots, x_{N-1}\}$$

and

$$\tilde{X} = \{\tilde{x}_0, \tilde{x}_1, \cdots, \tilde{x}_k, \cdots, \tilde{x}_{N-1}\}$$

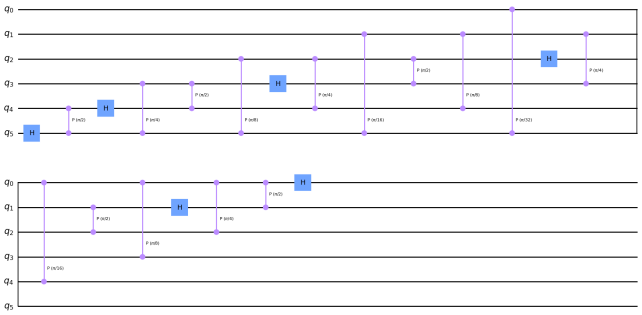

FIG. 3: the Quantum Fourier Transform for 6-qubit system

.

The discrete Fourier Transform, DFT, maps elements of X to elements of $\tilde{X}$, such that

$$\tilde{x}_k = \sum_{j=0}^{N-1} x_j\ \mathbf{e}^{2\pi\imath kj/N} \tag{25}$$

We can define the Quantum Fourier transform as

$$\begin{aligned} F|x\rangle &= \frac{1}{2^{n/2}} \sum_{k=0}^{N-1} \mathbf{e}^{2\pi\imath kj/2^n}|k\rangle \\ &= \frac{1}{2^{n/2}} \sum_{k_1=0}^{1} \cdots \sum_{k_n=0}^{1} \mathbf{e}^{2\pi\imath x\left(\sum_{l=1}^{n} k_l 2^{-l}\right)}|k_1\cdots k_n\rangle \\ &= \frac{1}{2^{n/2}} \sum_{k_1=0}^{1} \cdots \sum_{k_n=0}^{1} \bigotimes_{l=1}^{n} \mathbf{e}^{2\pi\imath x 2^{-l}}|k_l\rangle \\ &= \frac{1}{2^{n/2}} \bigotimes_{l=1}^{n} \left[\sum_{k_l=0}^{1} \mathbf{e}^{2\pi\imath x k_l 2^{-l}}|k_l\rangle\right] \\ &= \frac{1}{2^{n/2}} \bigotimes_{l=1}^{n} \left[|0\rangle + \mathbf{e}^{2\pi\imath x 2^{-l}}|1\rangle\right] \end{aligned} \tag{26}$$

We define

$$\phi_n = \frac{2\pi}{2^n} \tag{27}$$

Then, the Quantum Fourier Transfrom, F, can be implemented using Hadamard and controlled phase shift gates as shown in fig 3.

Then, Inverse Quantum Fourier Transform, $F^\dagger$, is implemented by a similar circuit, except, we make the transformation $\phi_n \to -\phi_n$. It is shown in fig 4

For $N = 2$, we have

$$\mathbf{e}^{-\imath x^2\Delta t/2m\hbar} = \mathbf{e}^{-\imath\tilde{\theta}_0 Z_0/2}\ \mathbf{e}^{-\imath\tilde{\theta}_{0,1}Z_0Z_1/2}\ \mathbf{e}^{-\imath\tilde{\theta}_1 Z_1/2} \tag{28}$$

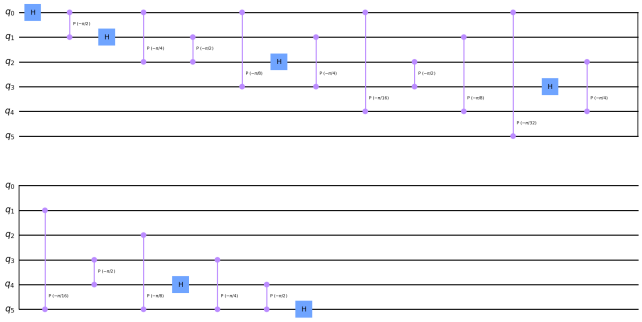

FIG. 4: Inverse Quantum Fourier Transform

where,

$$\tilde{\theta}_0 = -2(2\theta_{0,0}+2\theta_{0,1}+4\theta_0) = -2(2\theta_{0,0}+2\theta_{1,0}+4\theta_0) \quad (29)$$

$$\tilde{\theta}_{0,1} = 4\theta_{0,1} = 4\theta_{1,0} \quad (30)$$

$$\tilde{\theta}_1 = -2(2\theta_{1,1}+2\theta_{0,1}+4\theta_1) = -2(2\theta_{1,1}+2\theta_{1,0}+4\theta_1) \quad (31)$$

Recalling the transformation

$$\begin{aligned} &CX_{0,2}\,CX_{1,2}\,\mathbf{e}^{-\imath\theta Z_2}\,CX_{1,2}\,CX_{0,2} \\ &\qquad = \mathbf{e}^{CX_{0,2}\,CX_{1,2}\,Z_2\,CX_{1,2}\,CX_{0,2}} \\ &\qquad = \mathbf{e}^{-\imath\theta Z_0 Z_1} \end{aligned} \quad (32)$$

Then, Eq(24) becomes

$$\begin{aligned} &\mathbf{e}^{-\imath x^2 \Delta t/2m\hbar} \\ &= \mathbf{e}^{-\imath\tilde{\theta}_0 Z_0/2}\,CX_{0,2}\,CX_{1,2}\,\mathbf{e}^{-\imath\tilde{\theta}_{0,1} Z_2/2}\,CX_{1,2}\,CX_{0,2}\,\mathbf{e}^{-\imath\tilde{\theta}_1 Z_1/2} \end{aligned} \quad (33)$$

D. The time evolution circuit

The previous operators can be combined together to compose the goal evolution operator:

$$U(t)) = \text{QFT-1}e^{-\frac{i}{\hbar}(\frac{p^2}{2m})\Delta t}\text{QFT}^\dagger e^{-\frac{i}{\hbar}V(x)\Delta t}$$

which has the corresponding circuit (fig 5):

This is the evolution for just one time step. For several time steps, we repeat the one-time step circuit several times from the last step to the potential.

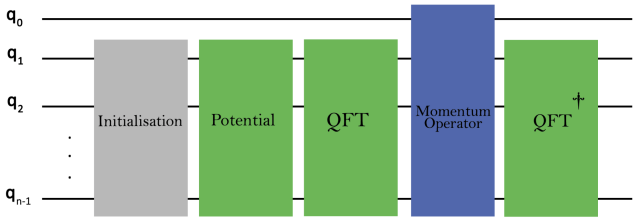

FIG. 5: Circuit diagram of time evolution

IV. EXPERIMENTS AND RESULTS

Using the above-defined algorithms and circuit design, we simulated the Schrodinger equation for 1-particle and 2-particle cases on the Statevector and QASM simulator. For 1 particle case, we have used 6 qubits, and for 2 particle case, we have used 8 quibts (4 for each).To initialize wave Gaussian wave is used for each case.

Position independent potentials: Consider a quantum particle in a constant potential

$$V(x) = V_0 \quad (34)$$

Hence, the potential operator becomes

$$\mathbf{e}^{-\imath V(x)\Delta t/\hbar} = \mathbf{e}^{-\imath V_0 \Delta t/\hbar} \quad (35)$$

which is a global phase to be ignored. Therfore, the potential operator for a particle in constant potential will be composed of one layer of identity gates applied on all the qubits.

The eigenstates for a particle in a step potential are Gaussian wavepackets multiplied by a factor of $\mathbf{e}^{ipx}$

$$\psi(x) = \frac{1}{\sigma\sqrt{2\pi}}\mathbf{e}^{-\frac{1}{2}\left(\frac{x-\mu}{\sigma}\right)^2}\mathbf{e}^{ipx} \quad (36)$$

The term $\mathbf{e}^{-\frac{1}{2}\left(\frac{x-\mu}{\sigma}\right)^2}$ represents the transmitted wave while the term $\mathbf{e}^{ipx}$ represents the reflected wave. For the free particle $p = 0$ and the state will be fully transmitted.

A. Free Particle

The free particle simulation is probably one of the easier quantum system to simulate, since it has no potentials, i.e. V = 0. We start of by initialising a Gaussian wave packet in the position-space of the form given in fig 6,

In the case of a free particle system, where the potential energy is zero, only the kinetic energy term contributes to the evolution equation. We conducted simulations of a free particle system using 6 qubits, taking care to minimize discretization errors. In each simulation, we ensured that the results closely matched those predicted by

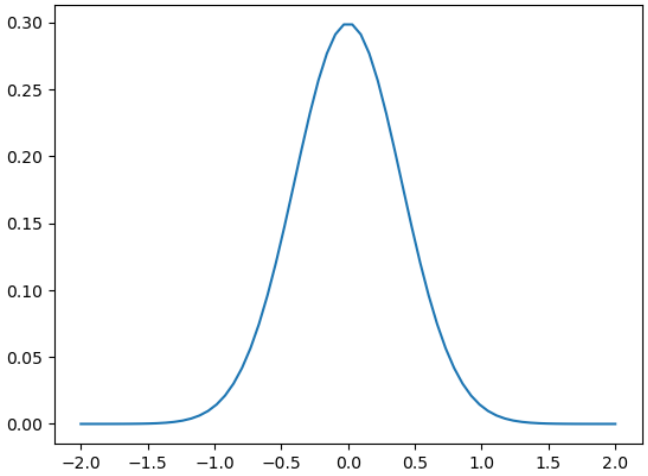

FIG. 6: The Gaussian curve that will be initialised onto the qubits, with $\mu = 0$ and $\sigma = 0.4$

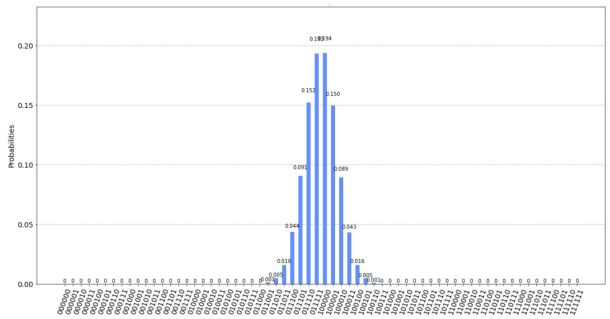

FIG. 7: Probability density plot at initialization step

quantum mechanics. Since there is no potential operator involved, we utilized a single time step for the simulation, as there was no need to divide the time into smaller intervals. The simulation result for different number of iteration can be seen in fig 7 8 9.

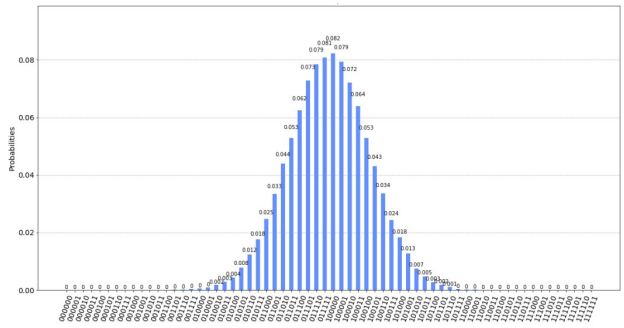

FIG. 8: Probability density plot at t=1

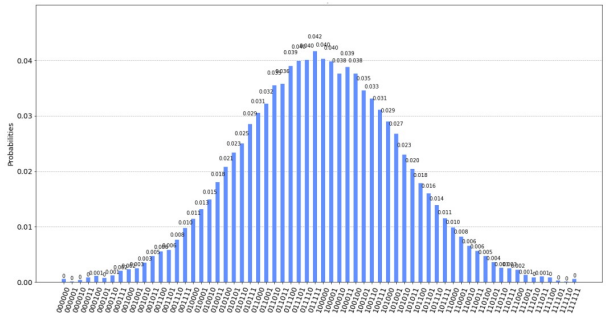

FIG. 9: Probability density plot at t=8

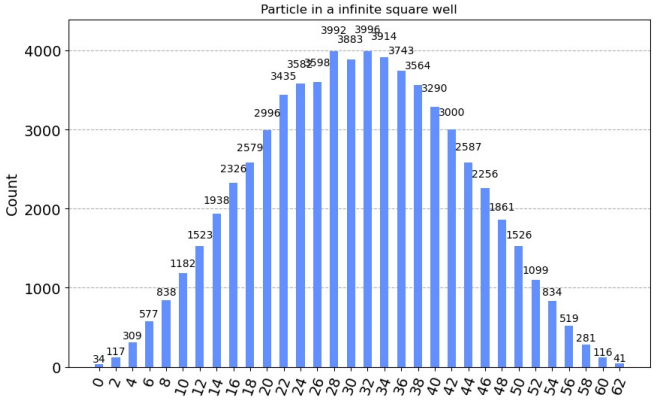

FIG. 10: Initial state

B. Particle in Square potential well

For infinite potential well, the potential is given by,

$$V(x) = \begin{cases} \infty; & x < 0 \\ 0; & 0 \leq x \leq L \\ \infty; & x > L \end{cases} \tag{38}$$

From Schrodinger equation solution ,the eigenstates for a particle in an infinite potential well is given by :

$$\psi_n(x) = \sqrt{\frac{2}{L}} \sin\left(\frac{n\pi x}{L}\right); \quad n \text{ is an integer} \tag{39}$$

For initialization, we extend the computational basis to be $0 \leq x \leq L$. We then add a phase gate, with V = 1000,L=1 at the highest order qubit, to define a step potential in ends. This mimics an infinite well and ensures that there will be no tunneling. Using the time-step of $\delta t = 0.01$, we simulated the results for many iterations. Due to the time evolution of the state, we can see the reflection of the wave from the potential wall but no tunneling, as expected for our case (fig 10 -12).

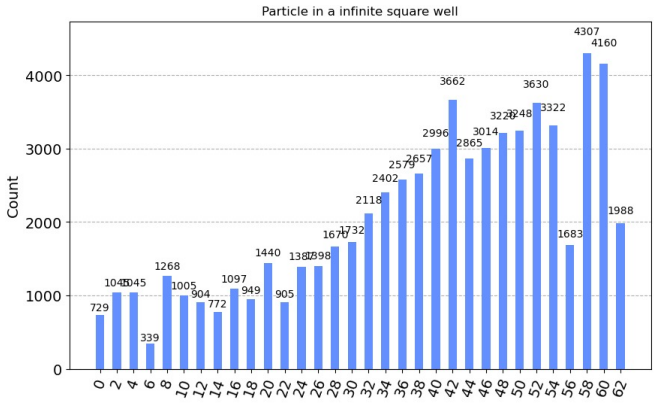

FIG. 11: After 3rd iteration

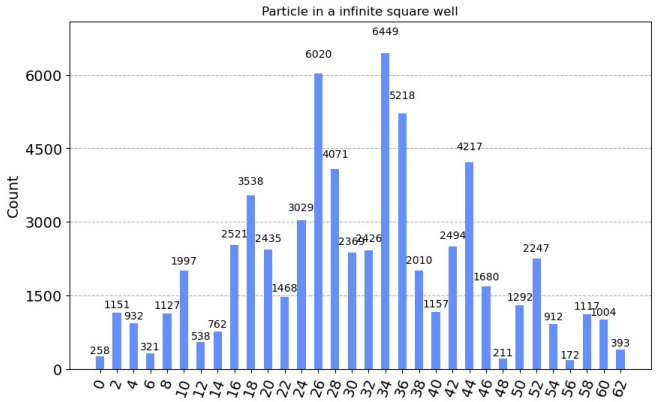

FIG. 12: After 7th iteration

C. Quantum Tunneling

We set the momentum to be p = 100 and L=1. Setting up a lower potential barrier for infinite square well condition. As the previous example, we set μ = 0 and =0.4, and $-2 \leq x \leq 2$. This ensures that the wave packet is initialized away from the potential barrier. We applied a thin barrier at x=0. See fig (13-14) for evolution. In Fig 15, we can see how initial wave packet tunnels and evolves from blue to red.

D. Simple Harmonic potential

The quantum simple harmonic oscillator is a fundamental system in quantum mechanics, often used to illustrate various quantum phenomena. It describes a particle (e.g., an electron) moving in a potential well that resembles the classical simple harmonic oscillator potential.

The Hamiltonian operator for the quantum harmonic oscillator is given by:

$$\hat{H} = \frac{\hat{p}^2}{2m} + \frac{1}{2}m\omega^2\hat{x}^2$$

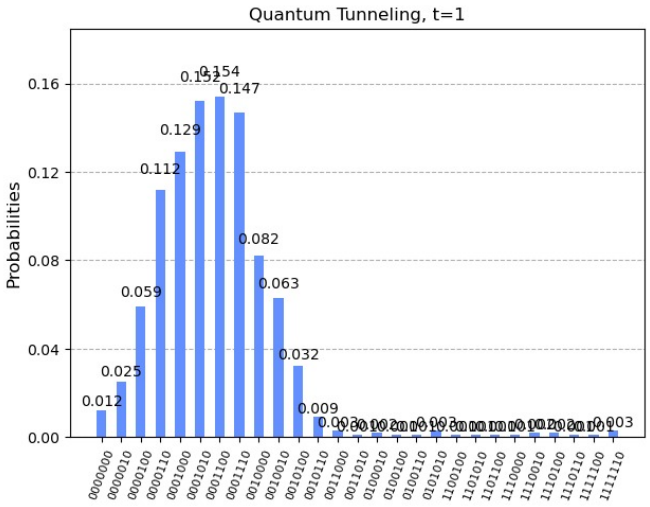

FIG. 13: Initial state after applying barrier potential

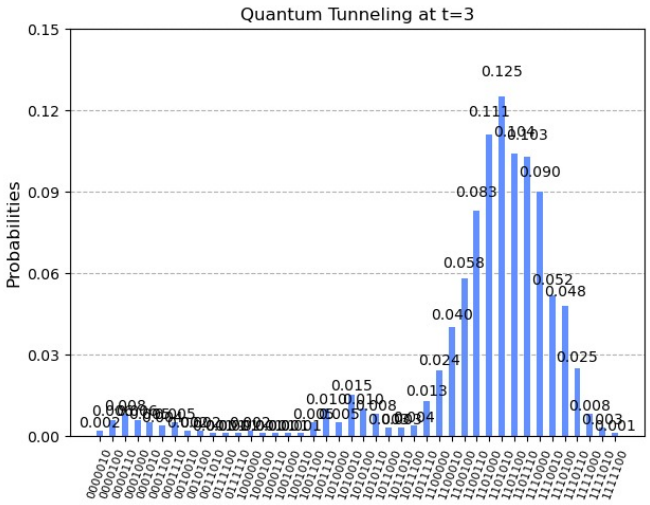

FIG. 14: 3rd iteration

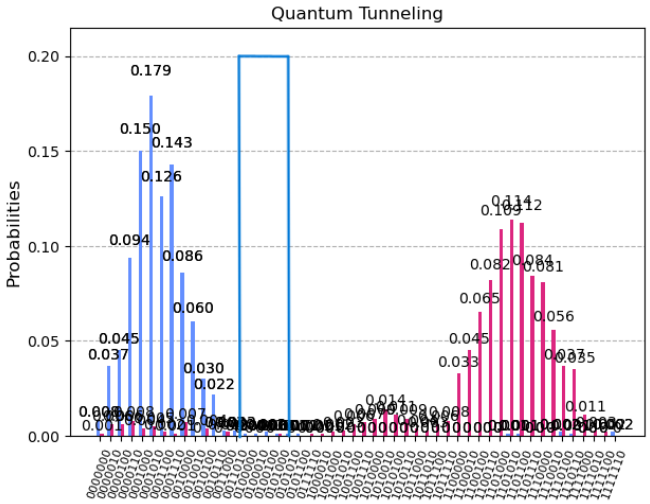

FIG. 15: initial state and 4th iteration

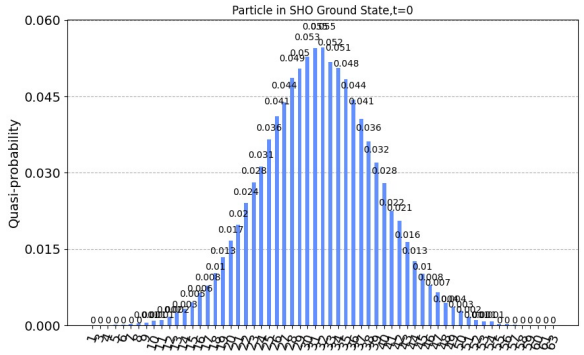

FIG. 16: Initial State

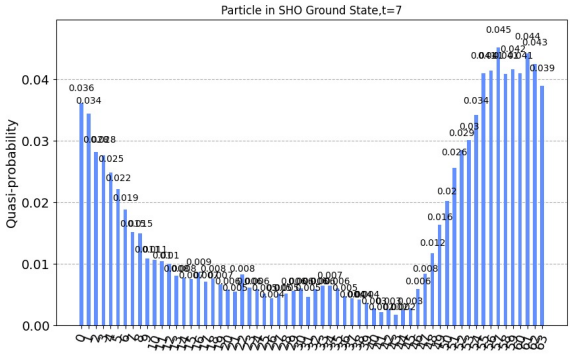

FIG. 17: 1st Iteration

where $\hat{p}$ is the momentum operator, $\hat{x}$ is the position operator, m is the mass of the particle, and ω is the angular frequency of the oscillator.

The time-independent Schrödinger equation for the harmonic oscillator is:

$$\hat{H}\psi_n(x) = E_n\psi_n(x)$$

where $\psi_n(x)$ is the wave function corresponding to the n-th energy eigenstate, and E_n is the corresponding energy eigenvalue.

The wave functions of the harmonic oscillator are given by the Hermite polynomials multiplied by a Gaussian factor:

$$\psi_n(x) = \left(\frac{m\omega}{\pi\hbar}\right)^{1/4} \frac{1}{\sqrt{2^n n!}} H_n\left(\sqrt{\frac{m\omega}{\hbar}}x\right) e^{-\frac{m\omega x^2}{2\hbar}}$$

where $H_n(x)$ are the Hermite polynomials, and $\hbar$ is the reduced Planck constant.

The energy eigenvalues of the harmonic oscillator are given by:

$$E_n = \left(n + \frac{1}{2}\right)\hbar\omega$$

where $n = 0, 1, 2, \ldots$ represents the quantum number associated with the energy levels. See Fig (16-19)

E. Two Interacting Schrödinger Particles

The Schrödinger equation for two interacting particles is given by:

$$i\hbar\tfrac{d}{dt}\psi_{AB}(x_A, x_B, t) = (H_{0A} + H_{0B} + V_A(x_A) + V_B(x_B) + V_{AB}(x_A - x_B))\psi_{AB}(x_A, x_B, t),$$

where x_A and x_B represent the position coordinates of the first and second particle, respectively. The operators $H_{0A} = \frac{p_A^2}{2m_A} = -\frac{\hbar^2}{2m_A}\frac{\partial^2}{\partial x_A^2}$ and $H_{0B} = \frac{p_B^2}{2m_B} = -\frac{\hbar^2}{2m_B}\frac{\partial^2}{\partial x_B^2}$ are the standard free Hamiltonians for the particles. The

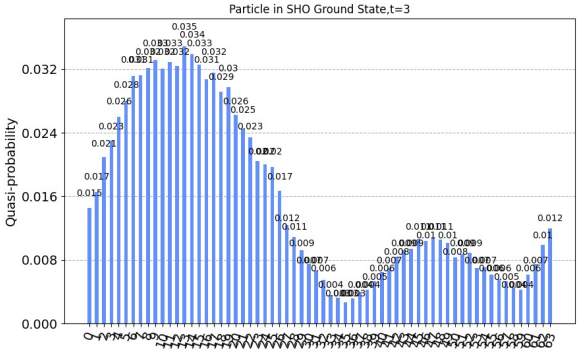

FIG. 18: 3rd Iteration

potentials $V_A(x_A)$ and $V_B(x_B)$ are external potentials affecting particles A and B respectively. The key potential V_{AB}, which accounts for the interaction between the particles, depends on the relative distance $x_A - x_B$. In this case, the interaction potential is modeled by a Dirac delta function, $V_{AB}(x_A - x_B) = v_0\delta(x_A - x_B)$, where v_0 is a constant.

The formal solution to this equation can be expressed

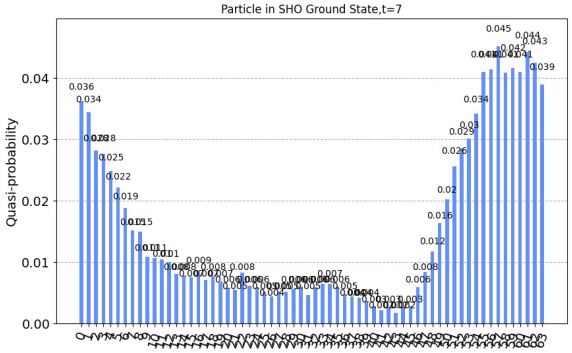

FIG. 19: 7th Iteration

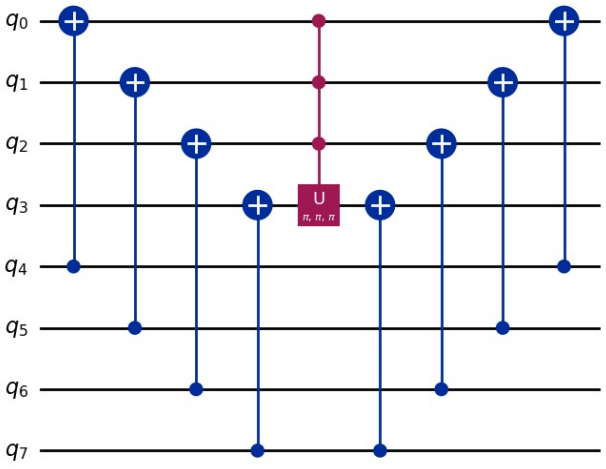

FIG. 20: Two particle interaction potential

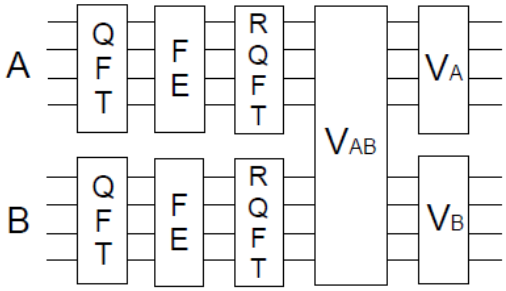

FIG. 21: Quantum Circuit for Two-Particle Case

as:

$$\psi_{AB}(x_A, x_B, t_1) = \exp\left(-\frac{i}{\hbar}\left(H_{0A} + H_{0B} + V_A(x_A) + V_B(x_B) + V_{AB}(x_A - x_B)\right)\Delta t\right)\psi_{AB}(x_A, x_B, t_0),$$

which describes how the system evolves from an initial state at time t_0 to a state at $t_1 = t_0 + \Delta t$. For the two-particle case, we have taken two particles in square well potential($-4 \leq x \leq 4$). Each Particle is initialized using 4 qubits as a Gaussian wave packet at x=-2 and x=2. The equation is evolved in a timestep of $\delta t = 0.01$. As expected, with the evolution of time, two wave packets first come closer, then separate and go towards the wall, as the box is 1D, and particle state overlap is impossible. See fig. 22

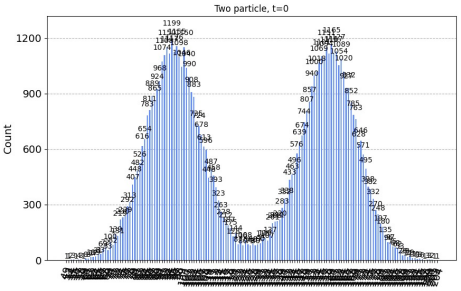

(a) Initial state

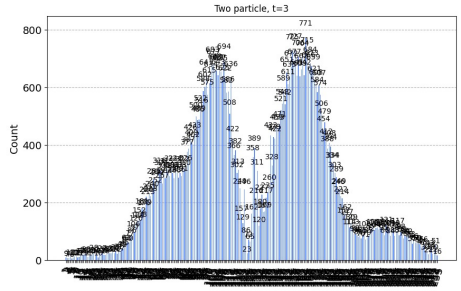

(b) 3rd iteration,

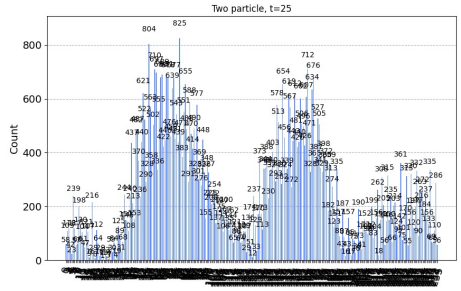

(c) 5th ietration

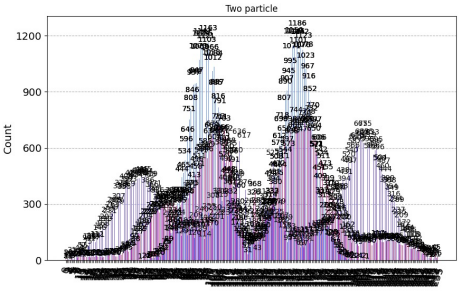

(d) All states

FIG. 22: Two particle Particle in infinite square well

V. CONCLUSION

Through our exploration, we've gained valuable insights into the behavior of quantum systems across various scenarios. Employing a quantum circuit and utilizing the QASM simulator, we delved into the behavior of particles, both individually and in pairs.

For the single-particle simulation, we utilized 6 qubits, while for the two-particle simulation, 8 qubits (4 each) were necessary. We initiated the particles' initial state using Gaussian waveforms, facilitating the representation of their quantum states within the simulation.

In addressing the infinite square well potential, we

adapted our setup to accommodate the periodic boundary of the simulation region. This necessitated expanding the computational basis and introducing a phase gate to emulate a step potential, mitigating tunneling effects.

In the scenario of a free particle system, devoid of potential energy, we streamlined the simulation by employing only one time step. This approach yielded results consistent with quantum mechanics predictions, as the beam's width expanded over time.

We also investigated the behavior of a quantum simple harmonic oscillator (SHO), a system commonly encountered in quantum mechanics. Our simulations revealed characteristic energy states and probability patterns associated with this potential, corroborated by comparison with the wavefunction of a known SHO.

Exploring quantum tunneling, where particles traverse barriers despite possessing less energy than the barrier itself, our simulations showcased the exponential decrease in the probability of finding the particle within the barrier, elucidating this unique quantum phenomenon. Our plots visually demonstrated the tunneling of the initial wave function to the opposite side.

Furthermore, we delved into the dynamics of two particles confined in a box, initially exhibiting distinct wave functions. As time elapsed, we observed the probability density of the particles merging and overlapping, eventually crossing each other and transitioning to the opposite side of the box.

Overall, our study underscores the prowess of quantum computing in simulating and comprehending intricate quantum systems. It not only presents opportunities for further research but also enriches our comprehension of the quantum realm.

VI. REFERENCES

1. Eltohfa, Mohamed, "Quantum Simulation of Schrödinger's Equation" (2021). Capstone and Graduation Projects. 23.

2. Abouelela, Mohamed, "Quantum Simulation of the Schrodinger Equation using IBM's Quantum Computers" (2020). Capstone and Graduation Projects. 20.

3. Benenti, G. and Casati, G. and Strini, G., "Principles Of Quantum Computation And Information - Volume Ii: Basic Tools And Special Topics"

4. M. Ostrowski, "Quantum simulation of two interacting schrodinger particles"